NOLTA, IEICE

Paper

Numerical analysis of bursting activity in an isolated pancreatic β-cell model

Hiroyasu Ando [1a)] *and Kantaro Fujiwara* [2b)]

[1] *Division of Policy and Planning Sciences, Faculty of Engineering, Information and Systems, University of Tsukuba 1-1-1 Ten-noudai, Tsukuba 305-8573, Japan*

[2] *Department of Management Science, Graduate School of Engineering, Tokyo University of Science 1-3 Kagurazaka, Shinjuku-ku, Tokyo 162-8601, Japan*

[a)] *ando@sk.tsukuba.ac.jp*
[b)] *kantaro@rs.tus.ac.jp*

Received August 20, 2015; Revised November 5, 2015; Published April 1, 2016

Abstract: Pancreatic β-cells exhibit bursting electrical activity, which is correlated with insulin secretion. It has been reported that several ionic channels may contribute to the characteristic electrical activities of these cells but their mechanisms are still unclear. In this study, we examined how the characteristic electrical activity of isolated β-cells occurs. Using a simple mathematical model of pancreatic β-cells, we found that conductances of the voltage-sensitive mixed ion channel and voltage-sensitive potassium channel contribute to such electrical activity. In addition, we found that noise can play a key role in this activity. These results imply that the bursting electrical activity of pancreatic β-cells can be controlled by ionic conductances or noise. Such control enables medical application of β-cells in type II diabetes, wherein insulin secretion is difficult to control. Our findings may contribute to a novel treatment for type II diabetes.

Key Words: pancreatic β-cell, burst, bifurcation, noise-induced oscillation

1. Introduction

Pancreatic β-cells are present in the islet of Langerhans. These cells secrete insulin, a hormone involved in glucose homeostasis for maintaining blood glucose level. They exhibit bursting electrical activity, which is correlated with insulin secretion. In both mice [1] and humans [2], insulin secretion is controlled by calcium oscillations. Calcium oscillations are driven by bursts of action potentials with periods ranging from tens of seconds to several minutes. However, it still remains elusive how such bursts arise and how they are modulated by glucose and other signals.

β-Cells in clustered intact islets exhibit regular bursting [3, 4]. In contrast, isolated single β-cells in rats show continuous spikes with shrinking amplitude [5]. Considerable experimental evidence indicates that the bursting activity of β-cells in islets depends on gap junctional couplings [6]. Although these couplings obviously contribute to β-cell bursting in islets, it is still unclear how continuous spikes

Nonlinear Theory and Its Applications, IEICE, vol. 7, no. 2, pp. 217–225 DOI: 10.1587/nolta.7.217

with shrinking amplitude occur in isolated cells.

In [5], the membrane potential of β-cells is recorded under glucose-stimulated conditions. At a low glucose concentration level, the membrane potential of isolated β-cells is at a resting potential, that is approximately -70 mV. By increasing the glucose concentration level, the membrane potential of isolated β-cells gradually increases and the cells finally emit burst-like spikes. The spike has three characteristics: continuous spikes, shrinking amplitude, and oscillation with small amplitude. In neuronal adaptation, neurons show reduction in their spike response, while adapting to the stimulus [7]. However, the amplitude is almost constant in neuronal adaptation, whereas it shrinks in β-cells adapting to the stimulus.

In this study, we examined how such characteristic spiking of isolated β-cells occurs. We have shown the effects of ionic conductances on the continuous spiking in isolated β-cells by using a simple mathematical model. Mathematical modeling of β-cells has contributed to the understanding of the mechanisms underlying β-cell activity, and several mathematical models that can reproduce the electrical activity of pancreatic β-cells have been proposed [8, 9]. In this study, we used the Chay model [9] which is a conductance-based model of membrane potential and consists of three variables. The model has been employed in many studies and is known to be a standard and simple model that can reproduce the characteristic bursting patterns of β-cells.

In Sec. 2, we have introduced the mathematical model that was used in this study. In Sec. 3, we have shown that the characteristic spiking of β-cells can be explained by modulation of the ionic conductances with noise. In Sec. 4, bifurcation analysis of the model has been described and noise-induced oscillation has also been analyzed. In Sec. 5, the physiological interpretation of our study has been discussed and the possibility of diabetes interventions has also been discussed.

2. Model

As a simple example of the bursting activity in β cells, we consider the model proposed by Chay, which is a conductance-based model of membrane potential [9]:

$$\begin{aligned}
\dot{V} &= g_{\mathrm{I}}^* m_\infty^3 h_\infty (V_{\mathrm{I}} - V) + g_{\mathrm{K,V}}^* n^4 (V_{\mathrm{K}} - V) \\
&\quad + g_{\mathrm{K,C}}^* \frac{C}{1+C} (V_{\mathrm{K}} - V) + g_{\mathrm{L}}^* (V_{\mathrm{L}} - V), \qquad (1) \\
\dot{n} &= (n_\infty - n)/\tau_n, \qquad (2) \\
\dot{C} &= \rho[m_\infty^3 h_\infty (V_{\mathrm{C}} - V) - k_{\mathrm{C}} C]. \qquad (3)
\end{aligned}$$

Equation (1) represents the dynamics of the membrane potential V, where V_{I}, V_{K} and V_{L} are the reversal potentials for mixed Na^+ and Ca^{2+}, K^+ and leakage ions, respectively. C is the concentration of intracellular Ca^{2+} ions divided by its dissociation constant from the receptor. g_{I}^*, $g_{\mathrm{K,V}}^*$, $g_{\mathrm{K,C}}^*$ and g_{L}^* are the maximal conductances divided by the membrane capacitance, where the subscripts (I), (K, V), (K, C) and (L) refer to the voltage-sensitive mixed ion channel, voltage-sensitive K^+ channel, Ca^{2+}-sensitive K^+ channel, and leakage channel, respectively. m_∞ and h_∞ are the probabilities of activation and inactivation of the mixed channel, respectively.

In Eq. (2), the dynamical variable n is the probability of opening in the voltage-sensitive K^+-channel, where τ_n is the relaxation time and n_∞ is the steady state value of n.

Note that the variables m_∞, h_∞, and n_∞ are replaced by the steady states described by $y_\infty = \alpha_y/(\alpha_y + \beta_y)$, where y stands for m, n, or h with

$$\begin{aligned}
\alpha_m &= 0.1(25+V)/[1-\exp(-0.1V-2.5)], \\
\beta_m &= 4\exp[-(V+50)/18], \\
\alpha_h &= 0.07\exp(-0.05V-2.5), \\
\beta_h &= 1/[1+\exp(-0.1V-2)], \\
\alpha_n &= 0.01(20+V)/[1-\exp(-0.1V-2)], \\
\beta_n &= 0.125\exp[-(V+30)/80].
\end{aligned}$$

Furthermore, τ_n is defined as

$$\tau_n = [230(\alpha_n + \beta_n)]^{-1}.$$

In Eq. (3), the dynamics of C is described, where $k_{\rm C}$, ρ and $V_{\rm C}$ are the rate constant for the efflux of intracellular Ca^{2+} ions, a proportionality constant and the reversal potential for Ca^{2+} ions, respectively. In Table I, we show the values of the parameters.

Table I. Parameters used in the numerical simulations.

Parameter	Value	Unit
$V_{\rm K}$	-75	mV
$V_{\rm I}$	100	mV
$V_{\rm L}$	-40	mV
$V_{\rm C}$	100	mV
$g^*_{\rm K,C}$	11	mV
$g^*_{\rm L}$	7	s^{-1}
$k_{\rm C}$	3.3/18	mV

3. Simulations

In this section, we have demonstrated numerical simulations of the model introduced in the previous section. Specifically, we have tried to qualitatively reproduce the experimental results reported by Yoshida *et al.* [5] by using the model with variations in the parameters $g^*_{\rm I}$ and ρ. In the following simulations, the parameter $g^*_{\rm K,V} = 1200$ is fixed.

First, we have shown results without noise in the model. Figure 1(a) at the parameter $g^*_{\rm I} = 1100$ shows periodic bursts in which the amplitude of the spikes in each bursting period is shrinking. Such a shrinking property in the bursting spikes was observed in the experiment in [5]. Moreover, the amplitude of the spikes finally vanished in each bursting period. In contrast, the amplitude did not vanish in each bursting period when $g^*_{\rm I} = 1200$, as shown in Fig. 1(b). Then, with increase in the value of $g^*_{\rm I}$, the shrinking property changed: the amplitude of spikes in each bursting period shank at first and then remained almost constant in the rest of the bursting period. Finally, at the value of $g^*_{\rm I} = 1300$, the amplitude of spikes shrank and then expanded in each bursting period as shown in Fig. 1(c). The bursting mechanism in terms of dynamical systems will be explained in the next section. In addition, Fig. 1(d) shows the power spectra of the time series in Fig. 1(a)–(c) for the period of one burst. In the figure, slightly wide peaks can be observed at almost the same frequency of ≈ 0.03 Hz. We confirmed that the frequency represents that of the spikes in the bursting period.

Next, we consider the case with noise in Eq. (1) as follows:

$$\begin{aligned}\dot{V} &= g^*_{\rm I} m^3_\infty h_\infty (V_{\rm I} - V) + g^*_{\rm K,V} n^4 (V_{\rm K} - V) \\ &\quad + g^*_{\rm K,C} \frac{C}{1+C}(V_{\rm K} - V) + g^*_{\rm L}(V_{\rm L} - V) + D\xi,\end{aligned}$$

where D is the strength of noise and ξ is white Gaussian noise following $N(0,1)$. We change the value of ρ as 0.03 which is smaller than that in the previous simulations. Figure 2(a) shows the time series of V with regard to $D = 10$, $g^*_{\rm I} = 1100$, and $g^*_{\rm K,V} = 1200$. As can be seen in the figure, the bursting period is prolonged compared to that in Fig. 1(a). The prolonged bursting period with noise and smaller value of ρ qualitatively reproduce the experimental result better than the previous simulations in Fig. 1. Note that the vanished spikes in the case without noise reappear as small oscillations due to noise as shown in Fig. 2(b). The mechanism of the noise induced oscillation will be discussed in detail in the next section.

4. Analysis

First, we consider the change in the bursting patterns in Fig. 1. As mentioned above, the amplitude of spikes in the bursting period shrinks; it vanishes at $g^*_{\rm I} = 1100$. The mechanism underlying the

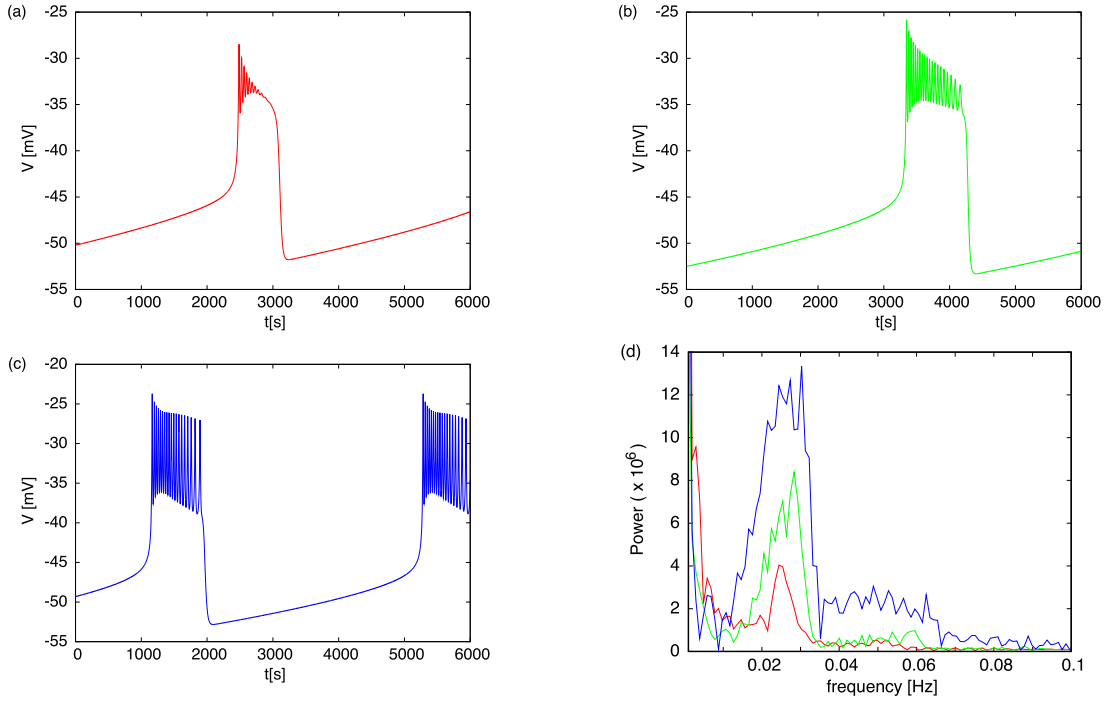

Fig. 1. Time series of V in the model with the parameters as $g_{\mathrm{I}}^{*} = 1100$ (a) (red), 1200 (b) (green), or 1300 (c) (blue), along with $g_{\mathrm{K,V}}^{*} = 1200$ and $\rho = 0.27$. (d) Power spectrum regarding the time series (a), (b), and (c) in the period of one burst. The color represents the corresponding g_{I}^{*}.

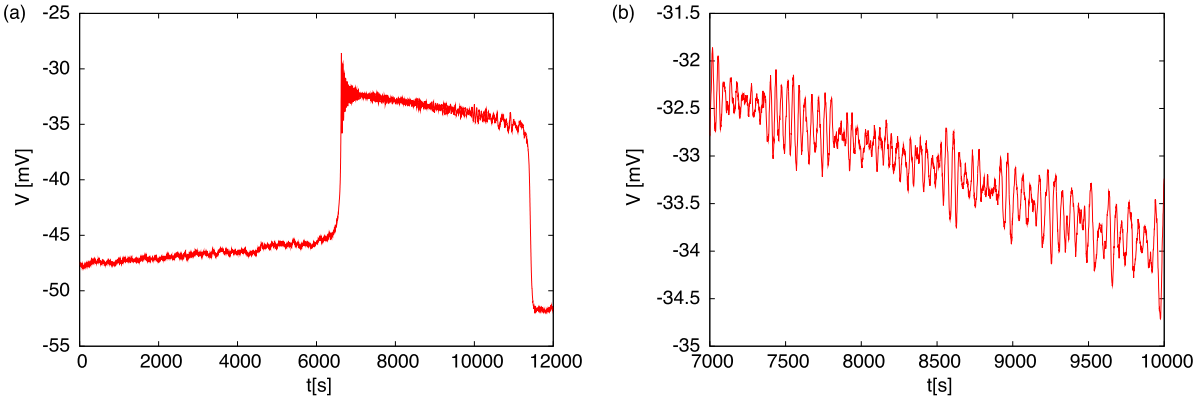

Fig. 2. (a) Time series of V in the model with the parameters as $g_{\mathrm{I}}^{*} = 1100$, $g_{\mathrm{K,V}}^{*} = 1200$, and $\rho = 0.03$ with noise $D = 10$. (b) Enlarged view of Fig. (a).

shrinking of the burst could be inferred from the bifurcation structure of the system described by Eqs. (1)–(3) with regard to the variable C as a bifurcation parameter. In [10], "Fold/Fold" bursting is defined as a trajectory in an attractor, which is similar to the red scroll attractor of the present system in Fig. 3(a). The trajectory for the smaller V and n represents the resting (or DOWN) state and that for the larger V and n corresponds to the bursting period. In the bursting period, we observed rotations of the trajectory for the lower value of C, and the rotation shrank and disappeared for the higher value of C. In [10], it was reported that the jump from the DOWN state to the bursting state is due to a fold bifurcation and the shrinking rotation is due to the damped oscillation as a transient of converging to the UP state, i.e., depolarized state without spiking. This is because the rate of attraction to the UP state is relatively weak compared to that of variation of C. Note that there are no limit cycles in the UP state. Thus, the trajectory jump from the UP state to the DOWN state is due to a fold bifurcation.

The bifurcation structures are illustrated in Fig. 3(b)–(d). The figures show the nullclines for V and n with trajectories provided that C is considered as a parameter. Figure 3(b) with $C = 0.3$ ((d)

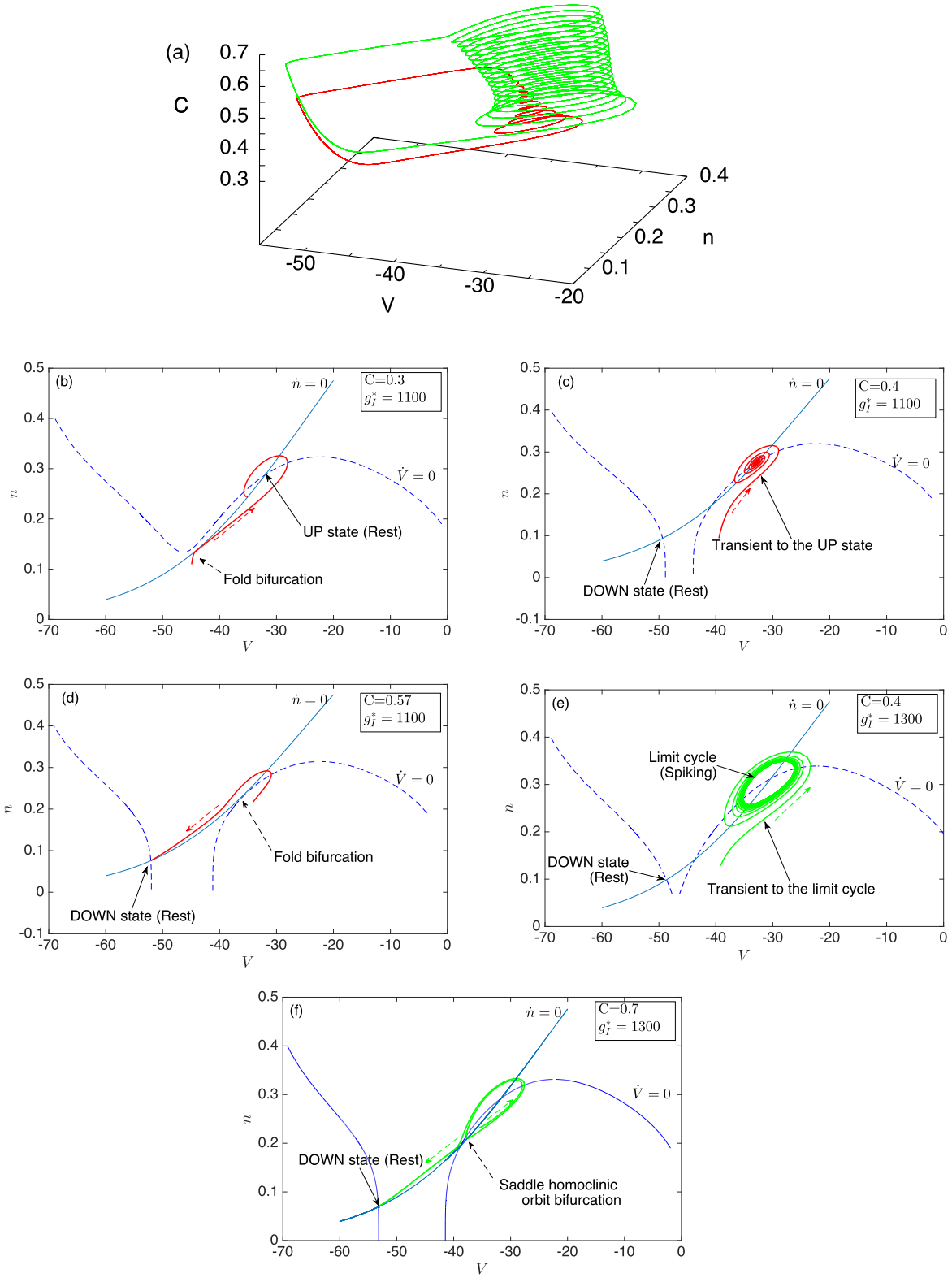

Fig. 3. (a) Attractor of the system (1)–(3) with regard to $g_{\mathrm{I}}^* = 1100$ (red) and $g_{\mathrm{I}}^* = 1300$ (green), and $g_{\mathrm{K,V}}^* = 1200$. $\rho = 0.27$. (b)–(e) Null clines and the trajectories at fixed C, namely, $C = 0.3$ (b), 0.4 (c), and 0.57 (d) for $g_{\mathrm{I}}^* = 1100$ and $C = 0.4$ (e) for $g_{\mathrm{I}}^* = 1300$.

with $C = 0.57$) indicates the fold bifurcation for the jump from the DOWN (UP) state to the bursting (DOWN) state. Figure 3(c) with $C = 0.4$ shows the transient of converging to the UP state. The convergence is so slow that the bursting behavior can be observed before the oscillation is damped.

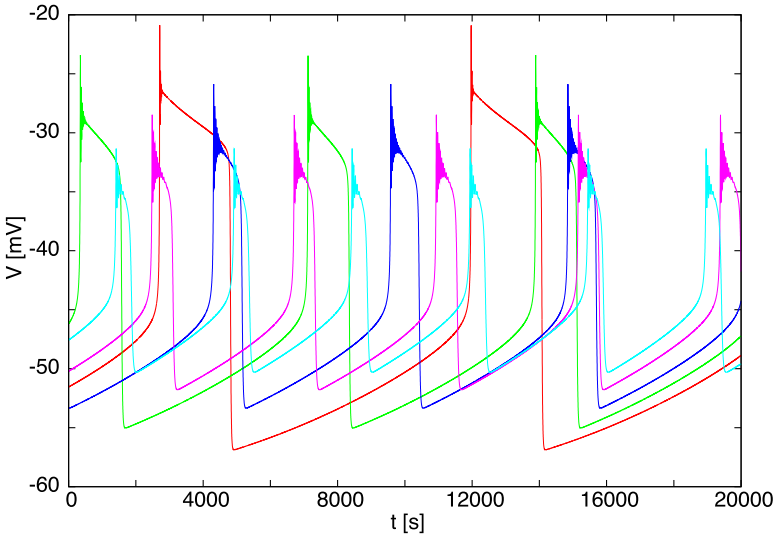

Fig. 4. Time series of V in the model with the parameters as $g_{\mathrm{I}}^{*} = 1100$ and $g_{\mathrm{K,V}}^{*} = 600$ (red), 800 (green), 1000 (blue), 1200 (magenta), or 1400 (light blue). $\rho = 0.27$.

For the parameter $g_{\mathrm{I}}^{*} = 1300$ in Fig. 1(c), we observed spikes in the whole bursting period without disappearing spikes. The corresponding attractor is shown in the green scroll in Fig. 3(a). The remaining spikes occured because there is a limit cycle in the bursting state which is not transient to the UP state. The limit cycle in the bursting period is shown in Fig. 3(e) for the fixed value of $C = 0.4$. Moreover, we observed shrinking spikes at the beginning of the burst as shown in Fig. 1(c). This is also due to the slow convergence to the limit cycle as can be seen from the trajectory in Fig. 3(e). Then, the jump from the DOWN (bursting) state to the bursting (DOWN) state is due to the fold bifurcation (the saddle homoclinic orbit bifurcation). Specifically, the trajectory representing the saddle homoclinic orbit is shown in Fig. 3(f).

Next, we investigated the change in bursting patterns when we fixed the value of g_{I}^{*} and varied the value of $g_{\mathrm{K,V}}^{*}$. We have shown the time series of V when we changed the value of $g_{\mathrm{K,V}}^{*}$ from 600 to 1400 while fixing $g_{\mathrm{I}}^{*} = 1100$ in Fig. 4. As can be seen in the figure, the length of the UP state becomes shorter with increase in the value of $g_{\mathrm{K,V}}^{*}$. In addition, the bursting frequency, namely the number of bursts in a fixed time interval, increased with increase in $g_{\mathrm{K,V}}^{*}$.

Finally, in order to investigate the phenomenon observed in Fig. 2(a), we performed frequency analysis of the oscillation in the UP state of the time series of V with and without noise. We set the parameter values as $g_{\mathrm{I}}^{*} = 1100$, $g_{\mathrm{K,V}}^{*} = 900$, and $\rho = 0.03$ with noise strength $D = 10$. Figure 5(a) shows the time series with (green) and without noise (red). We observe noise-induced oscillation at a similar frequency to that of the first several spikes in the case without noise, as shown in Fig. 5(a). In order to confirm the observation, the power spectra of those time series were calculated and are shown in Fig. 5(b). There is a peak in the power spectrum in each case. The frequency of the peak in the case without noise is accordance with the first several spikes in the bursting period. On the other hand, the peak in the case with noise is not in accordance with the first several spikes but corresponds to the oscillations after the spikes. This is because we omitted the first several spikes when we calculated the power spectrum. Note that the power spectrum for noise is averaged over 1000 realizations. Consequently, we confirmed that the frequency of the noise induced oscillation was similar to that of the first several spikes in the bursting period without noise.

5. Discussion

In pancreatic β-cells isolated from rats, continuous spikes with shrinking amplitude are observed [5], but the mechanism underlying this is still unknown. Our result implies that such characteristic spiking can be reproduced by modulating parameter values of the conductances of the voltage-sensitive mixed ion channel and voltage-sensitive potassium channel. When their values are in a certain range,

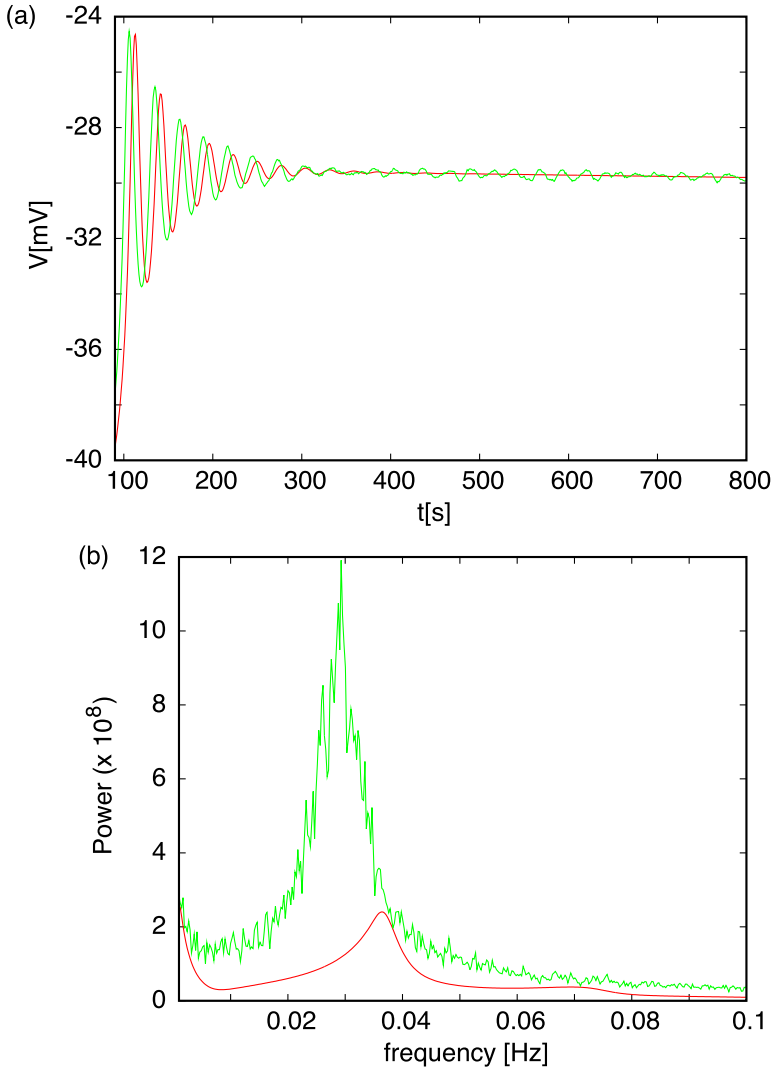

Fig. 5. (a) Time series with the parameters as $g_{\mathrm{I}}^{*} = 1100$ and $g_{\mathrm{K,V}}^{*} = 900$ with noise strength $D = 10$ (green) and without noise (red). $\rho = 0.03$. (b) Power spectrum for the time series with noise in the bursting period after the first several spikes (green) and without noise including the first several spikes (red). In the case with noise, the result is averaged over 1000 realizations.

characteristic spiking, as reported in [5], can be observed. By decreasing the proportionality constant of the calcium concentration, the period of the spiking is prolonged. These findings are obviously different from those for neuronal adaptation. In neuronal adaptation, the spiking amplitude is almost constant, while the amplitude shrinks in an isolated β-cell. Moreover, spiking frequency decreases considerably in neuronal adaptation, while the decrease in spiking frequency for an isolated β-cell is very slight. These different characteristics regarding adaptation to stimulus could be due to the differences in the adaptation mechanism: the calcium-dependent potassium current plays a key role [7] in neuronal adaptation, while voltage-sensitive mixed potassium and mixed currents play a major role in the adaptation of isolated β-cells. In addition, in the presence of additive noise, the spiking showed a noise-induced oscillation, which contributes to prolonging spikes with small amplitude in the bursting period. These findings indicate that the modulation of conductance values of the voltage-sensitive mixed ion channel, voltage-sensitive potassium channel and the proportionality constant of the calcium concentration under noisy conditions can explain the characteristic bursting in an isolated pancreatic β-cell.

It is known that, in a pancreatic β-cell in type II diabetes, decrease in bursting frequency leads to decrease in insulin secretion [11]. Our findings from the numerical simulations showed that the bursting frequency can be controlled to obtain an appropriate value by modulating the conductance

rates and noise. Therefore, it would be possible to apply our control scheme to a pancreatic β-cell in type II diabetes. For example, dendrotoxin is an inhibitor that inactivates voltage-sensitive potassium channels [12]. By using such inhibitors, the conductance rates of pancreatic β-cells can be controlled experimentally. From previous mathematical studies, it is known that bursting periods can be prolonged by increasing the glucose level, i.e., injecting high-amplitude input [8]. However, in most diabetic pancreatic β-cells, there is insensitivity to a high blood glucose level [13], which leads to insulin resistance [14] in type II diabetes. In such a case, it is considerably difficult to prolong the bursting period by increasing the glucose level [13]. On the other hand, our proposed mechanism of prolonging the bursting period does not depend on the glucose level, and only depends on the membrane conductance or noise level. This means that our proposed mechanism is applicable to pancreatic β-cells in type II diabetes, whose electrical activity is difficult to control. Our findings of an appropriate range of conductances may contribute to a novel treatment for type II diabetes.

Acknowledgments

This work is partly supported by a JSPS Grant-in-Aid for Challenging Exploratory Research (No. 15K12137). HA thanks CSTI, Cross-ministerial Strategic Innovation Promotion Program (SIP), "Next-generation power electronics" (NEDO). The authors are grateful to Prof. M. Kakei and Prof. M. Yoshida for their valuable suggestions.

References

[1] F.M. Ashcroft and P. Rorsman, "Electrophysiology of the pancreatic β-cell," *Prog. Biophys. Mol. Biol.*, vol. 54, pp. 87–143, 1989.

[2] F. Martin and B. Soria B, "Glucose-induced [Ca2+]i oscillations in single human pancreatic islets," *Cell Calcium*, vol. 20, pp. 409–414, 1996.

[3] E. Andreu, B. Soria, and J.V. Sanchez-Andres, "Oscillation of gap junction electrical coupling in the mouse pancreatic islets of Langerhans," *J. Physiol.*, vol. 498, pp. 753–761, 1997.

[4] P. Smolen, J. Rinzel, and A. Sherman, "Why pancreatic islets burst but single beta cells do not. The heterogeneity hypothesis," *Biophys. J.*, vol. 64, pp. 1668–1680, 1993.

[5] M. Yoshida, M. Nakata, S. Yamato, K. Dezaki, H. Sugawara, S. Ishikawa, M. Kawakami, T. Yada, and M. Kakei, "Voltage-dependent metabolic regulation of Kv2.1 channels in pancreatic β-cells," *Biochem. Biophys. Res. Commun.*, vol. 396, pp. 304–309, 2010.

[6] P. Rorsman and G. Trube, "Calcium and delayed potassium currents in mouse pancreatic β-cells under voltage-clamp conditions," *J Physiol.*, vol. 374, pp. 531–550, 1986.

[7] P. Pedarzani and J.F. Storm, "Pka mediates the effects of monoamine transmitters on the K+ current underlying the slow spike frequency adaptation in hippocampal neurons," *Neuron*, vol. 11, pp. 1023–1035, 1993.

[8] T.R. Chay and J. Keizer, "Minimal model for membrane oscillations in the pancreatic β-cell," *Biophys. J.*, vol. 42, pp. 181–190, 1983.

[9] T.R. Chay, "Chaos in a three-variable model of an excitable cell," *Physica D*, vol. 16, pp. 233–242, 1985.

[10] E.M. Izhikevich, "Neural excitability, spiking and bursting," *Int. J. Bifurcat. Chaos*, vol. 10, pp. 1171–1266, 2000.

[11] B. Colsoul, A. Schraenen, K. Lemaire, R. Quintens, L. Lommel, A. Segal, G. Owsianik, K. Talavera, T. Voets, R. Margolskee, Z. Kokrashvili, P. Gilon, B. Nilius, F. Schuit, and R. Vennekens, "Loss of high-frequency glucose-induced Ca2+ oscillations in pancreatic islets correlates with impaired glucose tolerance in Trpm5$^{-/-}$ mice," *Proc. Natl. Acad. Sci. USA.*, vol. 107, pp. 5208–5213, 2010.

[12] S. Gasparini, JM. Danse, A. Lecoq, S. Pinkasfeld, S. Zinn-Justin, L. Young, C. de Medeiros, E. Rowan, A. Harvey, and A. Ménez, "Delineation of the functional site of alpha-dendrotoxin. The functional topographies of dendrotoxins are different but share a conserved core with those of other Kv1 potassium channel-blocking toxins," *J. Biol. Chem.*, vol. 273, pp. 25393–25403, 1998.

[13] M.A. Abdul-Ghani, D. Tripathy, and R.A. DeFronzo, "Contributions of beta-cell dysfunction and insulin resistance to the pathogenesis of impaired glucose tolerance and impaired fasting glucose," *Diabetes Care*, vol. 29, pp. 1130–1139, 2006.

[14] H.K. Chiu, E. Tsai, R. Juneja, J. Stiever, B. Brooks-Worrell, A. Goel, and J. Palmer, "Equivalent insulin resistance in latent autoimmune diabetes in adults (LADA) and type 2 diabetic patients," *Diabetes Res. Clin. Pract.*, vol. 77, pp. 237–244, 2007.